

Proton-Proton Collisions at 3.5 GeV (*).

R. J. PISERCHIO and R. M. KALBACH

Department of Physics, University of Arizona - Tucson, Ariz.

(ricevuto il 17 Maggio 1962)

Summary. — Ilford G-5 emulsions were exposed to an external, 3.5 GeV proton beam of the Berkeley Bevatron. A total of 1200 nuclear interactions of beam protons was located, of which 128 were identified as proton-proton collisions. Multiple scattering, blob density, range and angle measurements were employed to determine the cross-sections for elastic and inelastic interactions as well as the identities and center-of-mass system momenta and scattering angles of secondaries from inelastic proton-proton interactions. This analysis indicates a cross-section of (8.0 ± 2.4) mb for elastic events, (24.1 ± 2.9) mb for two-prong inelastic events, (7.9 ± 1.4) mb for four-prong events and (0.6 ± 0.3) mb for six-prong events. The mean charged pion multiplicity in inelastic interactions is 1.5 ± 0.2 and corresponds to an average degree of inelasticity of 0.45 ± 0.06 . Center-of-mass system angular distributions of charged secondaries from inelastic events display a peaking for small scattering angles which is most pronounced for protons and pions from events with low secondary multiplicity. Momentum and transverse momentum distributions of secondary protons and pions from inelastic events are presented and compared with the results at other energies. The angular distribution of elastically scattered protons is found to be in fair agreement with that predicted by a uniform optical model of radius $1.25 \cdot 10^{-13}$ cm and opacity 0.66.

1. — Introduction.

The availability of artificially accelerated protons with energies from 1 to 30 GeV has encouraged a number of investigations of proton-proton interactions in this energy range. The principal objective of such experiments is to provide an indication of the important features of high-energy nucleon-

(*) Assisted by a grant from the National Science Foundation.

nucleon collisions in which multiple meson production contributes significantly. Although the behavior of the total and elastic cross-sections in this energy region has been rather extensively investigated, the variation of the partial inelastic cross-sections, the multiplicity of secondary mesons, and the energy and angular distributions of secondary protons and pions with bombarding energy is less well known.

The objective of the present experiment is to add to the available information of this type at an energy intermediate to that of previous experiments. In order to minimize the effect of the inclusion of collisions with bound protons in the sample of events selected for analysis, only those interactions are considered which satisfy rather stringent criteria with respect to any evidence which is not consistent with interpretation as a proton-free proton collision. In addition, as a check on the effect of scanning efficiency, two independent scanning methods are employed.

2. - Experimental procedure.

2.1. *Exposure, development and scanning.* - A stack of 600 μm , Ilford G-5 emulsion pellicles was exposed to an external, 3.5 GeV proton beam of the Berkeley Bevatron. The stack was oriented so that the incident particles entered the edge of the stack and travelled approximately parallel to the emulsion surfaces. After mounting, the plates were processed by a modified procedure in which the warm stage of the standard temperature cycle technique was replaced by development for 4.5 hours at $(5.0 \pm 0.5)^\circ\text{C}$ in order to reduce the effect of spurious scattering and distortion on multiple scattering and angle measurements.

The plates were scanned both by following lightly ionizing secondaries «up-stream» to the point of interaction, as described previously⁽¹⁾, and by following incident proton tracks. All nuclear interactions located by both methods were initially divided into three groups according to the following criteria:

i) Clean even-prong events. - An even number of charged secondaries, no recoil blob at the point of interaction, no secondary α tracks, no proton with a laboratory scattering angle greater than 90° , and no secondary proton with a kinetic energy greater than that of an elastically scattered proton with the same scattering angle.

ii) Clean odd-prong events. - Same as i) except with an odd number of charged secondaries.

iii) Stars. - All nuclear interactions which satisfy neither i) nor ii).

(1) R. M. KALBACH, J. J. LORD and C. H. TSAO: *Phys. Rev.*, **113**, 325, 330 (1959).

Clean even-prong events include, in addition to collisions with free protons, collisions with bound protons which result in no visible evidence of nuclear excitation. Approximately 50% of such events are examples of proton-free proton collisions although it is not possible in general to identify individual examples of free collisions. It is assumed here, however, that the general features of inelastic proton-free proton interactions will be fairly well represented by clean even-prong events when the momentum of the incident proton is much greater than the average Fermi momentum of bound nucleons. Clean odd-prong events are considered only in order to make a statistical separation of free and bound proton-proton collisions for the purpose of estimating the cross-section for proton-free proton collisions.

2'2. *Analysis of the events.* – Clean even prong events were initially separated into elastic and inelastic events by applying the following criteria to all such events with two charged secondaries:

i) The incident proton track and the two secondary tracks must be coplanar.

ii) The laboratory scattering angles of the two secondary tracks must satisfy the relation:

$$(1) \quad \operatorname{tg} \theta_r \operatorname{tg} \theta_s = 1 - v^2/c^2,$$

where θ_s is the smaller and θ_r is the larger of the two scattering angles and v is the velocity of the center-of-mass system with respect to the laboratory system.

Deviations from requirements 2'2 i) and ii) will be caused by measurement error, initial scattering of secondary tracks, and possible Fermi momentum of the target proton as well as by the production of neutral particles in inelastic collisions. The separation of elastic and inelastic collisions is facilitated by defining a quantity δ for each clean two-prong event which is a measure of the combined deviations from these requirements and which is given by:

$$(2) \quad \delta = \{[\theta_s - \operatorname{tg}^{-1}(\operatorname{ctg} \theta_r/\gamma_c^2)]^2 + (\Delta\varphi)^2\}^{1/2},$$

where $\Delta\varphi$ is the space angle between the small-angle secondary and the plane defined by the incident and large-angle secondary and γ_c refers to the velocity of the center-of-mass system with respect to the laboratory system. An analysis of a type discussed previously ⁽¹⁾ indicates that in the present experi-

ment δ must be less than 1.6° for an event to be classified as a possible example of elastic proton-free proton scattering.

Charged secondaries from all clean even-prong events not satisfying the requirements for elastic scattering were subjected to a combination of angle, energy loss, multiple scattering and range measurements. The identity and momentum of secondaries which pass out of the emulsion was determined by the method of Kalbach *et al.* (1) from a combination of blob density and multiple scattering measurements. Secondaries which came to rest in the emulsions were identified by the track endings characteristic of protons and pions in emulsion and the corresponding energy obtained from range-energy relations for emulsion (2).

Measurements of second differences due to multiple scattering were made with a Koristka MS-2 scattering stage using cell lengths of 100, 250 and 500 μm . In order to correct the measured second differences for the effect of distortion, stage noise and reading error, scattering measurements were made on 3.5 GeV proton tracks, both with the cell lengths used to measure secondaries and with 50 μm cell lengths. If \bar{D}_m is the mean measured absolute second difference, \bar{D}_{ss} is the second difference due to spurious scattering, \bar{D}_n is the second difference due to stage noise and reading error, and \bar{D}_c is the second difference due to Coulomb scattering, and if these quantities are assumed to have Gaussian distributions, we have the relation:

$$(3) \quad \bar{D}_m^2 = \bar{D}_{ss}^2 + \bar{D}_n^2 + \bar{D}_c^2.$$

The Coulomb scattering second difference is related to the momentum times velocity of a given track by the relation (3):

$$(4) \quad pv = KZL^{\frac{3}{2}}/573 \bar{D}_c,$$

where pv is the momentum velocity in MeV, K_z is the scattering factor, Z is the atomic number of the moving particle, L is the cell length in μm , and \bar{D}_c is in μm . For measurements on beam tracks, \bar{D}_m , and pv are known and the contribution of spurious scattering and noise can therefore be estimated from eqs. (3) and (4) for any given cell length. The contribution of noise was estimated from similar measurements using 50 μm cells, for which spurious scattering is assumed negligible. For 500 μm cells, \bar{D}_{ss} was found to be 0.197 μm , \bar{D}_n was 0.075 μm , and K_z was taken to be 25.

(2) University of California Radiation Lab. Report UCRL 2426.

(3) P. H. FOWLER: *Phil. Mag.*, **41**, 169 (1950).

All data reduction, including the identification of the secondaries, calculation of momenta and transformation of scattering angles and momenta to the center-of-mass system, was carried out on an IBM 650 electronic computer.

2'3. *Evaluation of cross-sections.* - Partial cross-sections for proton-free proton collisions were determined both for the secondary scanning and for beam scanning. For secondary scanning, corrections for scanning efficiency, secondary multiplicity and collisions with bound protons are necessary in order to obtain the true relative numbers of proton-free proton collisions resulting in 2, 4 and 6 charged secondaries. The results of such an analysis, described previously by KALBACH *et al.* (1) and BLUE *et al.* (4), are given in Table I. The corresponding partial cross-sections, σ_i , which are given in Table I are obtained from the relation:

$$(5) \quad \sigma_i = (1.47)n_i\sigma_s/n_s,$$

where n_i is the corrected number of events of a particular type and n_s is the corrected number of stars located in the same scan of the plates. σ_s is the cross-section for star production determined from beam scanning as outlined below.

TABLE I. - *Analysis of the results of secondary scanning.*

	Number of charged secondaries				
	2 (elastic)	2 (inelastic)	4	6	Stars
Number of events located	5	46	24	3	718
Number of events corrected for scanning efficiency	8.75	80.5	42	5.25	1256
Number of events corrected for secondary multiplicity	8.75	40.0	11.52	0.87	603
Number of events corrected for bound collisions	6.12	19.6	6.14	0.44	603
Cross-section for free proton-proton collisions, mb	7.5	24.1	7.5	0.50	—

(4) M. H. BLUE, J. J. LORD, J. G. PARKS and C. H. TSAO: *Phys. Rev.*, **125**, 1386 (1962).

Partial cross-sections for beam scanning were found from the corresponding mean free paths, after correction for collisions with bound protons, from the relation:

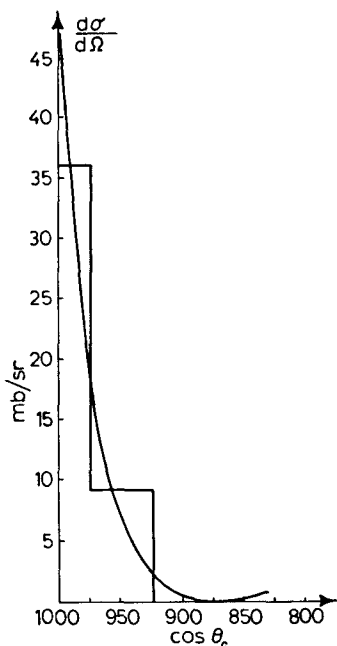
$$(6) \quad \sigma_i = 1/\lambda d,$$

where σ_i is the cross-section for a particular class of events, λ is the mean free path, and d is the density of free hydrogen in emulsion.

The results together with the corrections are shown in Table II.

TABLE II. - *Analysis of the results of beam scanning.*

	Number of charged secondaries				
	2 (elastic)	2 (inelastic)	4	6	Stars
Number of events located	6	21	7	1	329
Mean free path (meters)	23.6	6.7	20.2	141.6	0.42
Mean free path corrected for bound collisions	38.86	13.59	35.67	248	0.42
Cross-section, mb	8.5	24.1	9.19	1.1	506



3. - Results.

3.1. *Elastic collisions.* - The cross-sections for elastic scattering listed in Tables I and II are in slight disagreement, even considering the experimental errors. This is believed due to the difficulty of estimating the error due to scanning efficiency for small scattering angles in the case of the secondary scanning method. For this technique, the scanning efficiency drops rapidly to zero for scattering angles less than about 3° in the laboratory system, while

Fig. 1. - Center-of-mass system angular distribution of elastically scattered 3.5 GeV protons. The histogram represents the observed distribution while the curve represents the angular distribution of a uniform optical model of radius $R=1.25$ fermi, opacity $O=.66$, and $\Phi=0.0$.

the corresponding angle for beam scanning is less than 45'. A weighted average of these two results yields an elastic cross-section of (8.0 ± 2.4) mb. Figure 1 gives the center of mass system angular distribution of elastically scattered protons together with the predicted angular distribution of a purely absorbing optical disc whose parameters are computed from the experimental values of elastic and total cross-section calculated from beam scanning. This model has a radius of $1.25 \cdot 10^{-13}$ cm and an opacity of 0.66.

3'2. *Inelastic collisions.* - The best values for the partial inelastic cross-section, obtained from a weighted mean of the values from the two types of scanning are given in Table III. The resulting total cross-section is

TABLE III. - *Partial inelastic cross-sections.*

Number of secondary prongs	Cross-section, mb
2	24.1 ± 2.9
4	7.9 ± 1.4
6	0.6 ± 0.3

(40 ± 3.8) mb. In Table IV, a comparison of the partial inelastic cross-sections of the present experiment with those at several neighboring energies is given.

TABLE IV. - *Energy-dependence of partial inelastic cross-sections.*

Proton energy (GeV)	Partial cross-section in mb			
	2 prongs	4 prongs	6 prongs	8 prongs
6.15 ⁽¹⁾	7.3	12.1	2.7	0.3
4.15 ⁽⁴⁾	16.3	11.5	0.2	0.1
3.50 ⁽⁵⁾	24.1	7.9	0.6	—
2.75 ⁽⁶⁾	21.8	4.2	—	—
1.50 ⁽⁷⁾	25.9	1.1	—	—

The results of the present experiment are consistent with the observation of BLUE *et al.* ⁽⁴⁾ that the cross-section for inelastic events with two charged

⁽⁵⁾ Present work.

⁽⁶⁾ M. M. BLOCK *et al.*: *Phys. Rev.*, **103**, 1484 (1956).

⁽⁷⁾ W. B. FOWLER, R. P. SCHUTT, A. M. THORNDIKE and W. L. WHITTEMORE: *Phys. Rev.*, **103**, 1479 (1956).

secondaries decreases rapidly in the energy range from 1 to 6 GeV, while that for events with higher multiplicity suffers a corresponding increase in such a way that the total cross-section decreases slowly in this energy interval.

The present results may also be formulated to give the probabilities for the production of various numbers of charged pions in inelastic collisions. Table V gives these results and compares them with those at neighboring

TABLE V. - Probability, P_n , for the production of n charged pions as a function of bombarding energy.

	Bombarding energy, GeV			
	1.5 ⁽⁷⁾	2.75 ⁽⁶⁾	3.5 ⁽⁵⁾	6.2 ⁽¹⁾
P_0	4.9	9.3	14.6	9.4
P_1	74.5	66.6	44.9	41.5
P_2	15.7	13.3	22.5	15.1
P_3	4.9	10.7	14.6	9.4
P^4	—	—	3.4	17.0
P^5	—	—	—	1.9

energies. These results show a shift toward higher meson multiplicities which occurs as the bombarding energy increases from 1.5 to 6 GeV. In the

present experiment the mean charged meson multiplicity is found to be 1.5 ± 0.2 .

A total of 259 tracks from all inelastic events were identified as protons or pions. Figures 2 and 3 show the center-of-mass system momentum distribution for secondary protons and pions. The proton distribution shows a peak at a momentum of about 1.1 GeV/c with the mean value of 779 MeV/c (a kinetic energy of 350 MeV), while the peak of the pion distribution is at approximately 100 MeV/c with a mean value of 126 MeV/c (a kinetic energy of 48 MeV). The similarity of these distributions for two and four-prong

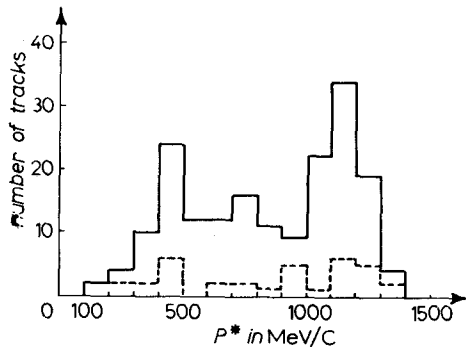


Fig. 2. - Momentum distribution of secondary protons from inelastic events plotted in the center-of-mass system (total of 107 tracks). The solid line is for all protons while the dashed line is for protons from 4-prong events.

events indicates a rough independence of the shape of this spectrum from secondary multiplicity. The shape of the pion spectrum is similar to that

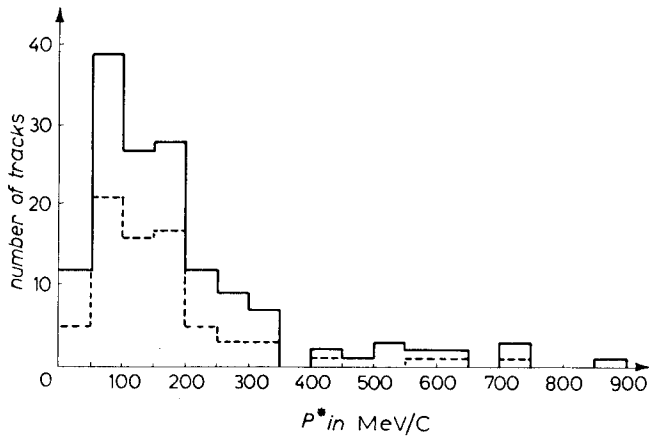


Fig. 3. - Momentum distribution of secondary pions from inelastic events plotted in the center-of-mass system (total of 155 tracks). The solid line is for all pions while the dashed line is for pions from 4-prong events.

derived by CERULUS *et al.* ^(8,9) at 2.75 and 6.2 GeV but is shifted to lower energies than predicted by this statistical theory.

The center of mass system angular distribution of secondary protons, shown

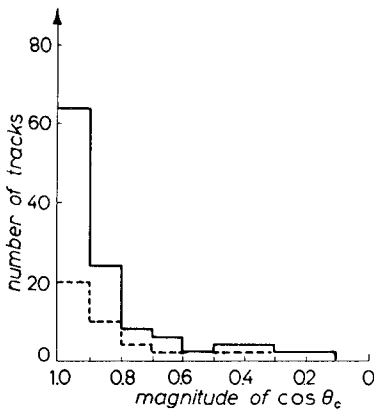


Fig. 4. - Center-of-mass system angular distribution of secondary pions from inelastic events (total of 155 tracks). The solid line is for all pions while the dashed one is for pions from 4-prong events.

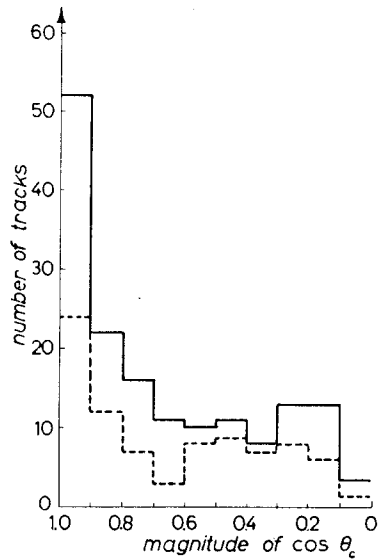


Fig. 5. - Center-of-mass system angular distribution of secondary protons from inelastic events (total of 107 tracks). The solid line is for all protons while the dashed line is for protons from 4-prong events.

⁽⁸⁾ F. CERULUS and R. HAGEDORN: CERN Report 59-3 (1959) (unpublished).

⁽⁹⁾ F. CERULUS and J. VON BEHR: *Nuovo Cimento*, **16**, 1046 (1960).

in Fig. 4, shows a definite tendency for emission at small scattering angles. A similar effect is indicated for secondary pions (Fig. 5) which is most pronounced for interactions with low secondary multiplicity.

These results suggest that events with high secondary multiplicity represent central collisions. The ratio of forward to backward scattering in the center-of-mass system is approximately 0.74. This is presumably due to inclusion of proton-bound proton collisions in the sample of events analysed as well as to statistical fluctuations and is of the same magnitude as reported elsewhere (^{1,4}).

Transverse momentum distributions for secondary protons and pions from inelastic events are shown in Fig. 6. The pronounced maxima between 0 and

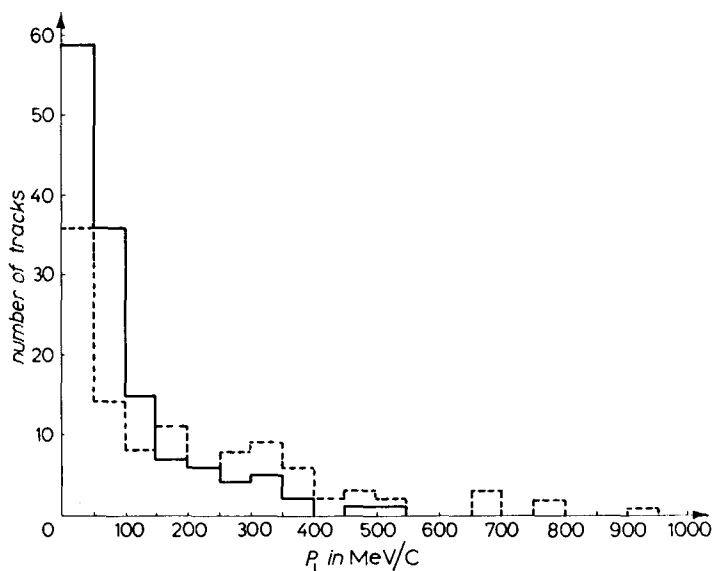


Fig. 6. - Transverse momentum distribution of protons (dashed line) and pions (solid line) from inelastic events.

50 MeV for both distributions may be compared with the observations of BLUE *et al.* (¹⁰) at 4.2 GeV, which indicate mean transverse momenta of 142 and 265 MeV/c for pions and protons, respectively, as compared to present values of 111 and 232 MeV/c.

An analysis of the Q -values for pairs of particles from inelastic 3.5 GeV proton-proton collisions together with similar analysis of such collisions at 19.8 GeV is presently in progress.

(¹⁰) M. H. BLUE, J. J. LORD, J. G. PARKS and C. H. TSAO: *Nuovo Cimento*, **20**, 274 (1961).

* * *

We wish to thank Mr. T. C. ANDREWS for providing data on proton-nucleus experiments. Grateful acknowledgment is also given to Miss CONNIE WOOTTEN for scanning, Mr. J. BARTH for general assistance, and Dr. M. MAHMOUD for interesting and helpful discussions. We are also indebted to Dr. W. CHUPP and the Bevatron staff for providing the exposure.

RIASSUNTO (*)

Si sono esposte emulsioni Ilford G-5 al fascio esterno di protoni di 3.5 GeV del Bevatrone di Berkeley. Si sono localizzate in totale 1200 interazioni nucleari di cui 128 si sono identificate come collisioni protoni-protoni. Si sono impiegate le misure dello scattering multiplo, della densità di blob, del range e degli angoli per determinare le sezioni d'urto per le interazioni elastiche ed anelastiche ed anche le identità, gli impulsi e gli angoli di scattering nel sistema del centro di massa dei secondari delle interazioni protone-protone anelastiche. Questa analisi indica una sezione d'urto di (8.0 ± 2.4) mb per gli eventi elastici, (24.1 ± 2.9) mb per gli eventi anelastici a due rami, (7.9 ± 1.4) mb per gli eventi a quattro rami e (0.6 ± 0.3) mb per quelli a sei rami. La molteplicità media dei pioni carichi nelle interazioni anelastiche è 1.5 ± 0.2 e corrisponde ad un grado medio di anelasticità di 0.45 ± 0.06 . Le distribuzioni angolari nel sistema del centro di massa dei secondari carichi da eventi anelastici presentano un picco per piccoli angoli di scattering che è più pronunciato per i protoni e i pioni da eventi con bassa molteplicità secondaria. Si presentano le distribuzioni dell'impulso e dell'impulso trasversale dei protoni e pioni secondari da eventi anelastici e si confrontano con i risultati ad altre energie. Si trova che la distribuzione angolare dei protoni con scattering elastico è in buon accordo con quella predetta da un modello ottico uniforme di raggio $1.25 \cdot 10^{-13}$ cm ed opacità 0.66.

(*) Traduzione a cura della Redazione.